Intrinsic Nucleation Mechanism and Disorder Effects in Polarization Switching on Ferroelectric Surfaces

Peter Maksymovych,[1,*] Stephen Jesse,[1] Mark Huijben,[2] Ramamoorthy Ramesh,[2] Anna Morozovska,[3]
Samrat Choudhury,[4] Long-Qing Chen,[4] Arthur P. Baddorf,[1] and Sergei V. Kalinin[1,†]

[1]*Center for Nanophase Materials Sciences, Oak Ridge National Laboratory, Oak Ridge, Tennessee, 37831, USA*
[2]*Department of Materials Sciences and Engineering and Department of Physics, University of California Berkeley,
Berkeley, California, 94720, USA*
[3]*V. Lashkaryov Institute for Semiconductor Physics, National Academy of Science of Ukraine, 41, pr. Nauki, 03028, Kiev, Ukraine*
[4]*Department of Materials Science and Engineering, Pennsylvania State University, University Park, Pennsylvania, 16802, USA*

The temperature dependence of ferroelectric domain nucleation in epitaxial films of $BiFeO_3$ is studied using variable temperature ultrahigh vacuum piezoresponse force spectroscopy in the 50 to 300 K temperature range. The nucleation bias corresponding to the onset of local ferroelectric switching in the volume of an electrostatic field confined by the metal tip was found to change less than 20% across the entire temperature range. A combination of the analytical and phase-field analysis proves that the weak temperature dependence of nucleation bias is a hallmark of an intrinsic nucleation mechanism with minimal contribution of thermal fluctuations. The effect of disorder on the observed distribution of the nucleation bias between vacuum and ambient environments is compared.

Ferroelectricity in low-dimensional materials, coupling between order parameters, and ferroelectric control of electronic transport [1] provide fertile opportunities to seek new materials, dynamics and device applications. Theoretically predicted behaviors in spatially confined ferroelectrics include transitions between toroidal and ordered ferroelectric states [2] and complex field-temperature phase diagrams in thin films [3]. The advances in theoretical understanding of nanoferroelectrics are currently in stark contrast to a relatively small number of experimental observations in such systems. It is therefore imperative to address the mechanism of ferroelectric switching in low-dimensional ferroelectrics, the polarization domain nucleation in confined geometries that approach the size of the critical nucleus, and the comparative role of domain nucleation and domain-wall motion in the switching process.

Traditional capacitor-based measurements have demonstrated the crossover from wall motion limited to nucleation limited regimes [4,5] and strong deviation from the Kolmogorov-Avrami-Ishibashi switching kinetics [6] when domain nucleation is rate-limiting [4]. When combined with scanning probe microscopy, such measurements can directly probe the position and density of the nucleation centers [7], nucleation statistics [8], and the speed of domain wall motion [5]. Similarly, time-resolved x-ray microdiffraction has been used to image the switching of a ferroelectric capacitor, identifying regions of faster switching in the nanosecond time regime [9]. However, the electric field is essentially uniform in a capacitor, resulting in rapid domain growth after the nucleation event and precluding systematic studies of domain nucleation and its variability within the material. In contrast, piezores-ponse force spectroscopy (PFS) [10], based on contact-mode atomic force microscopy, is a direct method to study local polarization dynamics and spatially resolved nucleation process [10,11], since the electrostatic field of the metal tip is highly localized, and the nanoscale domain nucleation under the tip is the limiting step in a PFS experiment.

The scope of this Letter is the mechanism of single domain nucleation in PFS. Most previous works assumed thermally activated nucleation because a large electric field under the tip can reduce the nucleation barrier to a thermally accessible value [12,13]. Recent phase-field simulations have suggested, however, that an *intrinsic* mechanism may also take place [14]. At the same time, the absolute values of the nucleation bias are strongly affected by poorly controlled parameters, such as the screening efficiency, which determines the depolarization energy of a nucleating domain [15] and the stability of the ferroelectric phase [16]. The lack of environmental control and the limited temperature range in ambient experiments have thus precluded the unambiguous determination of the nucleation mechanism, the activation energy of nucleation, and the elucidation of the properties of the critical nucleus.

We have studied temperature-dependent local ferroelectric switching under ultrahigh vacuum (UHV) over a wide temperature range from 50 to 300 K. The measurements were carried out using a commercial microscope (Omicron) modified for piezoresponse force microscopy (PFM) measurements at pressures $<2 \times 10^{-9}$ Torr. Piezoresponse of the ferroelectric surface was measured with the tip in contact mode, by sinusoidal excitation of the cantilever (Au, CSC37, Mikromasch) at its contact resonance (240–300 kHz). Local ferroelectric hysteresis loops

were obtained from 100-200 random locations on the surface away from major topographic defects using switching spectroscopy PFM [10]. The investigated samples were 50 and 200 nm thick epitaxial films of BiFeO$_3$(100) (BFO) grown by pulsed-laser deposition on SrTiO$_3$(100) (STO) buffered by a 50 nm conducting SrRuO$_3$ electrode. Cooling was achieved by a liquid helium flow cryostat connected to the sample holder via a copper braid. The reported temperatures (measured by a silicon diode) are lower by no more than 15 K of the substrate values. Given the very small temperature dependence of the hysteresis loops (see below), this systematic offset does not influence the conclusions of the Letter or the comparison with theory.

An out-of-plane PFM image of the BiFeO$_3$(100) surface and an average hysteresis loop obtained at 300 K in UHV are shown in Fig. 1. Although the domain structure itself does not change upon transition into vacuum, the hysteresis loop shifts to lower voltages by $\sim$1 V, and its shape is noticeably changed. The film is predominantly monodomain with the out-of-plane polarization pointing in the downward direction. The nucleation bias values (measured at the 3% of the total change of the piezoresponse signal during switching) on the 50 nm BFO sample are 1.1 $\pm$ 2.0 V and -3.6 ± 1.6 V. Such small values are characteristic of 180° ferroelectric switching since the ferroelastic regime (70.5° or 109° rotation) onsets at significantly higher voltages [17]. The evolution of the hysteresis loop with temperature obtained with the same probe and the corresponding statistics of the nucleation bias are shown in Fig. 2(a) and 2(b). The change of the nucleation bias is unexpectedly small and amounts to at most a 20% increase at 52 K, Fig. 2(c), while the temperature dependence of the nucleation bias is almost linear. This is in stark contrast to capacitor measurements where the coercive voltage is strongly temperature dependent [18]. The temperature dependence was reproduced using three different cantilevers with no noticeable deviations due to cantilever wear during the experiments.
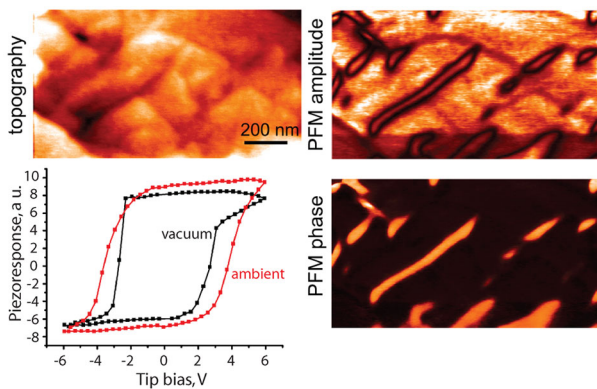
To understand the mechanism of the observed weak temperature dependence, we compare it to the predictions of the analytical solutions for the rigid ferroelectric [15] and the numerical phase-field modeling. Within the rigid model based on the Landauer approximation, the magnitude of polarization under the tip is independent of the electric field, with polarization values $+P_S$ far from the probe and $-P_S$ inside the semiellipsoidal domain. The domain wall is infinitely thin. The approximate expression for the free energy of the domain as a function of applied bias U is

$$E_a(U) \approx \frac{d^3}{12\varepsilon_0(\kappa + \varepsilon_e)P_S}\left(\frac{\pi\psi_S\gamma}{U}\right)^3, \qquad (1)$$

where ψ_S is domain-wall surface energy, d is the separation between the surface and the point charge that models the field of the biased probe, $\kappa = \sqrt{\varepsilon_{11}\varepsilon_{33}}$ is the effective
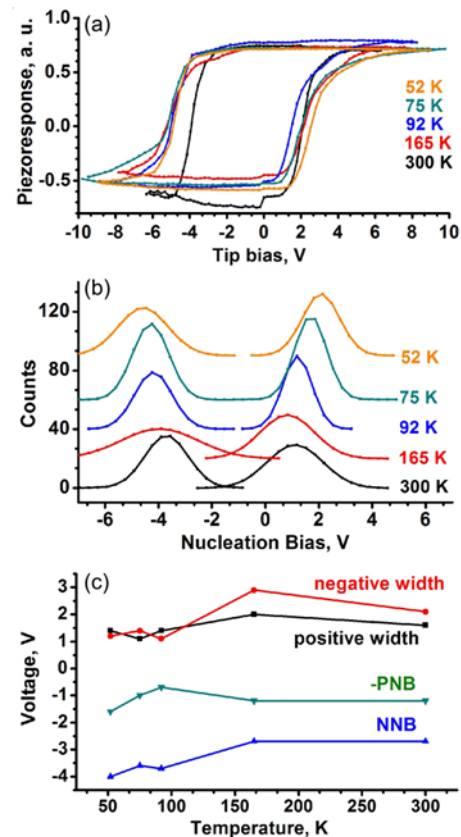

FIG. 2 (color online). Temperature dependence of local ferroelectric switching. (a) Average hysteresis loops of a 50 nm BiFeO$_3$ film as a function of sample temperature obtained using switching spectroscopy PFM in 100–200 places on the surface for each loop. A step feature around zero-bias is an experimental artifact. (b) Statistical distribution of nucleation bias shown as a Gaussian fit to the measured histograms. The nucleation bias for each local loop was measured as at 3% change of the total piezoresponse signal using a 9-parameter phenomenological fit to the experimental loop. (c) Temperature dependence of the nucleation bias (NNB for negative, PNB for positive) and the width of the distributions from (a) and (b), respectively.

FIG. 1 (color online). Topography, amplitude, and phase of piezoresponse of 50 nm BiFeO$_3$(100) film used in this study. The panel below shows averages of 50–100 local ferroelectric hysteresis loops obtained with the same physical cantilever in ultrahigh vacuum and after venting the chamber to ambient.

dielectric constant of ferroelectric material, $\gamma = \sqrt{\varepsilon_{33}/\varepsilon_{11}}$ is the dielectric anisotropy factor, and $\varepsilon_e = 1$ for vacuum. The temperature dependence of the ferroelectric parameters for the second order ferroelectrics is $P_S \sim \sqrt{T_C - T}$, $\psi_S \sim (T_C - T)^{3/2}$, $\varepsilon_{33} \sim |T_C - T|^{-1}$, for perovskites $\varepsilon_{11} \sim |T_C - T|^{-1}$, where T_C is the Curie temperature. The temperature dependence of the nucleation bias can then be estimated from the activation rate theory as $E_a(U_n) = m k_B T$ (m is an integer 1...25), thus determining when thermal fluctuations overcome the activation barrier. The final temperature dependence of the nucleation bias is $U_n \approx U_0 (T_c - T)^{5/3} T^{-1/3}$, where U_0 is a temperature-independent constant.

The switching process was also modeled using phase-field simulations [14] by numerically solving the time-dependent Landau-Ginzburg-Devonshire equation $\partial P_i(x, t)/\partial t = -M \delta F/\delta P_i(x, t)$ where M is a kinetic coefficient related to domain-wall mobility and F is a free energy functional, with material parameters from Ref. [19]. The in-plane lattice constants of $BiFeO_3$ are fixed to those of $SrTiO_3$. The nucleation bias was determined as the minimum applied electric potential for the onset of polarization switching.

To account for the influence of the tip size and the built-in field on the nucleation bias, we normalized the data to a relative scale $(\langle PNB \rangle + |\langle NNB \rangle|)_T / (\langle PNB \rangle + |\langle NNB \rangle|)_{300K}$, where $\langle PNB \rangle$ and $\langle NNB \rangle$ are the median values of the experimental distributions or the theoretical values for the positive and negative nucleation bias, respectively, at a temperature T. As seen in Fig. 3(a), the rigid model predicts a much stronger temperature dependence of the nucleation bias than that observed experimentally. In contrast, both the magnitude and linearity of the temperature dependence predicted by the phase-field modeling [Fig. 3(b)] are very close to the experiment. Unlike the rigid model, phase-field calculations do not include thermal fluctuations, thus probing the intrinsic switching regime. Therefore, this analysis strongly indicates that single-domain nucleation in the confined electric field of the AFM tip is indeed intrinsic, i.e., it proceeds via tilting of the ferroelectric double-well potential until one of the minima essentially vanishes in the critical volume. Nucleation will therefore occur even at 0 K, which is not permitted if the nucleation is thermally activated.

As seen in Fig. 3(b), the linear temperature dependence of the nucleation bias [$U_n(T) \approx U_0(T_C - T)$] is also predicted by the *analytical* model for intrinsic switching developed using a direct variational method [20,21]. This model considers an intrinsic (rather than infinitely thin) width of the domain wall and a variable (rather than rigid) magnitude of polarization. The small temperature dependence of the nucleation bias arises primarily from the temperature dependence of the dielectric constants and the spontaneous polarization. The conclusions derived here do not consider possible contributions of the antiferromagnetic order in the multiferroic $BiFeO_3$ since the piezo-
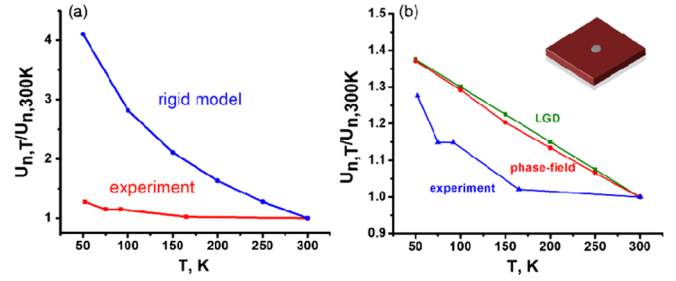

FIG. 3 (color online). Measured and calculated temperature dependence of the nucleation bias. The y-axis is a nucleation bias normalized to the room temperature values. (a) Comparison of experiment with rigid model; (b) Comparison of experiment with phase-field calculations and the analytical LGD model (see Supplementary information [21]). The values of the nucleation bias obtained from phase-field modeling of local ferroelectric switching on $BiFeO_3(100)$ using a Lorentzian distribution of electric field strength on the surface with a characteristic width of 25 nm. The numerical parameters for the LGD-based values ($T_c = 974$ K and $U_0 = -0.0077$ V/K) were obtained by fitting to phase-field data.

magnetic coupling was previously estimated to be negligibly small [22]. We also measured the temperature dependence on the nonmagnetic $Pb(Zr_{0.2}Ti_{0.8})O_3(100)/SrRuO_3/SrTiO_3$ and found that the average nucleation bias increased by ~ 1.4 on a 30 nm film upon cooling the film to 145 K. This difference is larger than the corresponding value for $BiFeO_3$ since the T_c of PZT is lower (~ 670 K). However, the observed increase is still significantly smaller than a factor of ~ 2.3 (or roughly 1.5^2) predicted by the rigid model for PZT.

While sequential hysteresis loops obtained at a single point are highly reproducible, the nucleation bias varies across the surface and follows a Gaussian distribution [Fig. 2(b)] with full width at half maximum of 1–2 V [Fig. 2(c)]. This variability stems from the inherent disorder, such as defects and defect concentration fluctuation, long-range elastic fields, correlated variations of the built-in field, as well as instrumental artifacts such as the variations in the contact area due to surface roughness [10]. To identify the dominant disorder components, we sampled 400 hysteresis loops from a random surface area on the 200 nm $BiFeO_3$ sample on a grid with 100 nm spatial resolution. We also repeated the measurements after venting the vacuum chamber to air, to investigate the possible effect of electrostatic boundary conditions on the observed disorder. The correlation between PNB and NNB is shown in Fig. 4 as a 2D probability distribution histogram. The hysteresis loops in vacuum are substantially imprinted on average, $\langle PNB \rangle = 0.2$ V and $\langle NNB \rangle = -2.5$ V [Fig. 4(a)], unlike those in ambient, $\langle PNB \rangle = 1.9$ V vs $\langle NNB \rangle = -1.8$ V [Fig. 4(b)]. At the same time, the scatter of PNB in vacuum is much smaller than that of NNB [Fig. 4(a) and 4(c)], while in ambient these values are nearly the same [Fig. 4(b) and 4(d)]. Therefore, it appears that the strong built-in field in vacuum causes the degree of
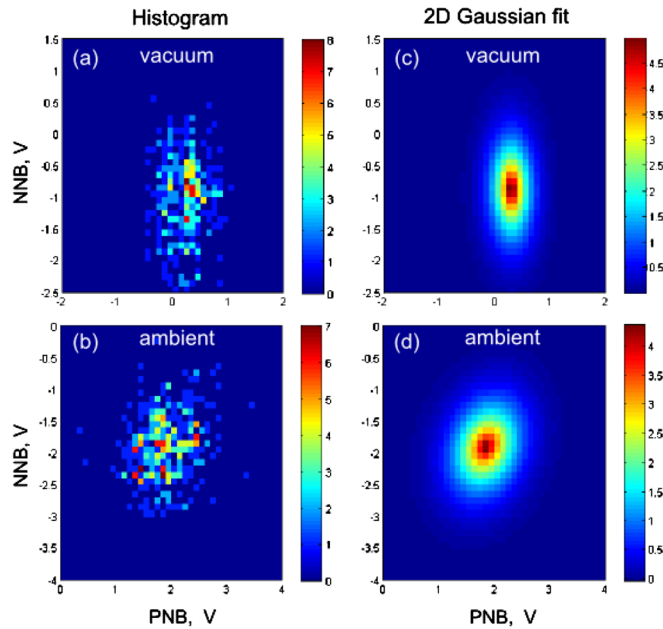
FIG. 4 (color online).   Statistical correlation between positive and negative nucleation bias measured on 200 nm $BiFeO_3$ film in vacuum and ambient environment. (a), (b) 2D-histograms of the nucleation bias values. (c), (d) 2D-Gaussian fits to the histograms in (a), (b), respectively.

disorder to be different for the opposite switching directions. We propose that the tilt of the ferroelectric double-well potential produces a different potential barrier to nucleation and correspondingly a different size of the critical nucleus for the opposite directions of ferroelectric switching. As a result, the geometric sampling of the built-in disorder will also be different. The almost perfect compensation of the built-in field in ambient symmetrizes the double-well potential and the nucleation process, yielding a nearly equal degree of disorder for the two switching directions. Note also that the 2D Gaussian fit to the histogram is slightly elongated along the 45° direction in ambient [Fig. 4(d)], indicating a small preference of the random-field disorder, where both nucleation voltages are shifted in the same (positive or negative) direction.

To summarize, based on the temperature dependence of local polarization switching on ferroelectric surfaces, we have established an intrinsic, as opposed to thermally activated, mechanism for single-domain nucleation in the confined electric field of the AFM tip. Theoretical modeling suggests that Landauer-like rigid ferroelectric models have limited applicability to the description of the local phase transitions because of the incorrect description of the potential energy saddle point. In a similar recent development, the Miller-Weinreich model was shown to overestimate the activation barriers to domain wall motion because of the rigid constraints on the critical nuclei [23]. Finally, based on the comparative analysis of the disorder in vacuum and ambient environment, we suggest that the built-in field across the film controls the critical size of the nucleus

for single-domain nucleation. These results will be pertinent to investigating the role of single defects on phase-transitions in ferroelectric materials, including the domain-wall pinning mechanisms as well as ferroic phase transitions in disordered materials. We also anticipate the general conclusions derived here to be applicable well beyond the model ferroelectric system toward other electric-field-induced phase transitions, such as solid state reactions and electrochemical transformations in molecular systems.

*Corresponding author: maksymovychp@ornl.gov
†sergei2@ornl.gov

[1] E. Y. Tsymbal and H. Kohlstedt, Science **313**, 181 (2006).
[2] S. Prosandeev, I. Ponomareva, I. Kornev, I. Naumov, and L. Bellaiche, Phys. Rev. Lett. **96**, 237601 (2006).
[3] A. M. Bratkovsky and A. P. Levanyuk, Phys. Rev. Lett. **94**, 107601 (2005).
[4] A. K. Tagantsev, I. Stolichnov, N. Setter, J. S. Cross, and M. Tsukada, Phys. Rev. B **66**, 214109 (2002).
[5] A. Gruverman, D. Wu, and J. F. Scott, Phys. Rev. Lett. **100**, 097601 (2008).
[6] H. Orihara, S. Hashimoto, and Y. Ishibashi, J. Phys. Soc. Jpn. **63**, 1031 (1994).
[7] A. Gruverman et al., Appl. Phys. Lett. **82**, 3071 (2003).
[8] J. Y. Jo et al., Phys. Rev. Lett. **99**, 267602 (2007).
[9] A. Grigoriev et al., Phys. Rev. Lett. **96**, 187601 (2006).
[10] S. Jesse et al., Nature Mater. **7**, 209 (2008).
[11] S. V. Kalinin et al., Phys. Rev. Lett. **100**, 155703 (2008).
[12] A. N. Morozovska et al., J. Appl. Phys. **102**, 114108 (2007).
[13] A. Y. Emelyanov, Phys. Rev. B **71**, 132102 (2005).
[14] S. Choudhury, Y. L. Li, C. E. Krill, and L. Q. Chen, Acta Mater. **53**, 5313 (2005).
[15] A. N. Morozovska et al., J. Appl. Phys. **102**, 114108 (2007).
[16] D. D. Fong et al., Phys. Rev. Lett. **96**, 127601 (2006).
[17] F. Zavaliche et al., Phase Transit. **79**, 991 (2006).
[18] L. Pintilie, I. Vrejoiu, D. Hesse, G. LeRhun, and M. Alexe, Phys. Rev. B **75**, 104103 (2007).
[19] J. X. Zhang et al., J. Appl. Phys. **103**, 094111 (2008).
[20] A. N. Morozovska, S. V. Kalinin, E. A. Eliseev, V. Gopalan, and S. V. Svechnikov, Phys. Rev. B **78**, 125407 (2008).
[21] See EPAPS Document No. E-PRLTAO-101-056848 for supplemental information. For more information on EPAPS, see http://www.aip.org/pubservs/epaps.html.
[22] S. V. Kalinin et al., Proc. Natl. Acad. Sci. U.S.A. **104**, 20204 (2007).
[23] Y. H. Shin, I. Grinberg, I. W. Chen, and A. M. Rappe, Nature (London) **449**, 881 (2007).